Journal of Al-Azhar University Engineering Sector

Vol.17, No. 63, April 2022, 577- 589

STUDYING THE COUPLING OF A CONCENTRATOR PHOTOVOLTAIC CELL WITH THERMOELECTRIC GENERATOR

Omar Emad [1*], Mohamed Emam [1], M.A. Abdelrahman [1], Ahmed A.A. Attia [1].

[1] Department of Mechanical Engineering, Shoubra Faculty of Engineering, Benha University, Egypt.

*Corresponding Author E-mail: omar.galal@feng.bu.edu.eg

Received: 12 Jan. 2022 Accepted: 14 Feb. 2022

ABSTRACT

Concentrator photovoltaic technology (CPV) use solar concentrators to maximize incident solar energy and hence create more electricity per unit area. However, increasing the solar incident irradiance raises the temperature of the solar cell and consequently reduces its efficiency. The current study uses the Thermo Electric Generator (TEG) as a passive cooling system to reduce the CPV surface temperature and use the waste heat energy to generate additional electricity. The study also compared the performance of a hybrid CPV-TEG to the baseline uncooled CPV. The results showed that under standard operating conditions, the uncooled MJ solar cell could not be exposed to solar radiation concentrations greater than 18.25 suns, with maximum electrical output of 0.7 W/cm^2. In contrast, the hybrid CPV/TEG system can operate at solar radiation concentrations up to 37.60 suns, and thus the resulting power is maximized to reach 1.433 W/cm^2.

Keywords: CPV, multijunction, solar cell, thermoelectric generation, CPV/TEG hybrid system.

دراسة اقتران الخلية الكهروضوئية المركزة مع المولد الكهروحراري

عمر عماد ١, محمد امام ١, محمد عبدالرحمن ١, احمد عطية ١.

١ قسم الهندسة الميكانيكية، كلية الهندسة بشبرا، جامعة بنها، مصر.

* * البريد الإلكتروني للمؤلف الرئيسي: omar.galal@feng.bu.edu.eg

الملخص

تستخدم التكنولوجيا الكهروضوئية المركزه الإشعاع الشمسي المركز لتعظيم كمية الطاقة الشمسية الواقعة وبالتالي إنتاج كمية اكبر من الكهرباء لكل وحدة مساحات و لكن مع زيادة تركيز الإشعاع الشمسي ترتفع درجة حرارة الخلية الشمسية وتنخفض كفاءتها .تستخدم الدراسة الحالية المولدات الكهروحراريه كنظام تبريد سلبي لتقليل درجة حرارة سطح الخليه الشمسيه المركزة واستخدام الطاقة الحرارية المهدرة لتوليد كهرباء إضافية ، كما اشتملت الدراسه علي مقارنة أداء النظام الهجين من الخلية الشمسية المركزة المبرده بواسطة مولد كهروحراري الي أداء الخلية الشمسية المركزة الغير مبرده. أظهرت النتائج أنه في ظل ظروف التشغيل القياسية ، لا يمكن أن تتعرض الخلية الشمسية متعددة الانويه غير المبردة لتركيزات إشعاع شمسي أكبر من ١٨,٢٥ شمس ، وبالتالي يبلغ الحد الأقصى لأنتجاها الكهربائي ٠,٧ وات/سم٢ في المقابل عندما يتم دمج الخلية الشمسية مع مولد

كهروحراري سيمكن الخلية أن تعمل بتركيزات إشعاع شمسي تصل إلى ٣٧,٦٠ شمس وبالتالي يتم تعظيم معدل انتاج الطاقه الكهربيه من النظام لتصل إلى ١,٤٣٣ وات/سم٢.

الكلمات المفتاحية : الخلاية الشمسية المركزه، الخلاية الشمسية متعددة الانوية، الخلاية الشمسية، المولد الكهروحراري، النظام الهجين للخلاية الشمسية المركزه/ المولد الكهروحراري.

1. INTRODUCTION

Solar energy is an infinitely abundant source of energy, making it one of the most favorable renewable energy sources [1]; the photoelectric effect is one of the techniques that utilize the incident solar radiation by direct conversion into electric energy using photovoltaic cell (PV-cells).

Many modifications were made to PV systems to boost cell power production. One of these techniques was using low-cost lenses and mirrors to make better use of the solar spectrum by concentrating it over the cell surface, which is known as a Concentrator photovoltaic system (CPV-system), the levels of solar concentration has categories between Low Concentration with CR< 10 suns, medium Concentration for 10<CR<100, High Concentration for 100< CR<1000 suns and Ultra-high Concentration for CR>1000 [2].

Multijunction solar cells were used to improve cell conversion efficiency, which use multiple cell layers stacked on top of each other with diode tunnels to interconnect those layers. This technology has increased cell efficiency to 46.1% by 2016 [3]. This is a significant improvement over single-junction cells, whose efficiency was limited to 12% to 18% [4].

A concentrator system with MJ cells creates an effective power generation system with high incident power and extended system efficiency, Figure 1 (a) shows an assembly of MJ solar cells array with concentrator Fresnel lens [5].

However, many problems arise at high solar concentration Most notably in cell temperature, which is overheated under such conditions, resulting in a decrease in cell efficiency by rates reaches 0.106% with each 1°C increase in cell temperature [6]. Cell cooling became necessary at high concentration ratios to avoid deterioration in cell efficiency.

CPV cooling techniques vary between active and passive. Active cooling relies on driving fluid over the cell surface using a pump or fan; however, this technique needs a constant power supply to deliver the needed power to run the system.

The passive system does not require input power from an external source and relies solely on free convection, evaporation, condensation, phase change materials, thermoelectric material, and other phenomena that do not rely on an external power source.

A thermoelectric generator (TEG) is a device composed of two different materials joined by a junction that converts heat into electric energy when a temperature gradient is introduced across its surface via a phenomenon known as the Seebeck effect [7].

In the last years, TEG has attracted more attention by using it in power generation from waste heat [8]; one of these applications was using TEG in CPV systems to use waste heat and offer an additional power source.

TEG offers various advantages as a power generation source since it is a static system with no moving parts, creates no pollutants, does not undergo any chemical reactions, and has many other benefits [7], one of commercially used TEG made of Bismuth telluride (Bi_2Te_3) is shown in Figure 1 (b) [8].

Usage of the thermoelectric generator as a passive cooling technique experimentally and numerically, Liao T et al. [9] conducted an experimental test to assess the cooling impact on the PV system with the TEG cold side attached to the cooling water basin, and the findings revealed a 25% increase in system efficiency above the PV cell efficiency, Sabry M et al. [10] also performed experimental studies as well using CPV cell of dimensions 10×10 mm^2 with TEG on its bottom surface, the TEG cold ceramic immersed in cold water at 20 °C, and the results showed that for the 40×40 mm^2 The system efficiency would increase by 5.8%, While Deng Y et al. [11] employed Matlab software to compare the CPV/TEG hybrid system to the concentrator polycrystalline-Si photovoltaic cell, the results showed that the hybrid system delivered a 14 % improvement over the CPV system alone, Beeri O et al. [12] also performed numerical analysis using finite element modeling to assess the performance of a CPV-TEG system with the controlled bottom of TEG cold ceramic at a temperature of 30 °C, and the results showed that solar concentration ratio of 200 suns the hybrid system overall efficiency increased to 40%.

Fewer studies have been conducted on using the simple construction of only CPV/TEG with TEG surfaces exposed to ambient conditions without an additional complex cooling source, and this passively cooled system creates a hybrid power generation system that uses waste heat from the CPV as an auxiliary power generation source by the TEG.

The current study aims to investigate the performance of a hybrid triple-junction concentrator solar cell with a thermoelectric generator attached to its bottom surface using 3D simulation software. The analysis is accomplished by comparing the hybrid system's performance against uncooled triple-junction cells over a medium solar concentration range with the same ambient conditions.

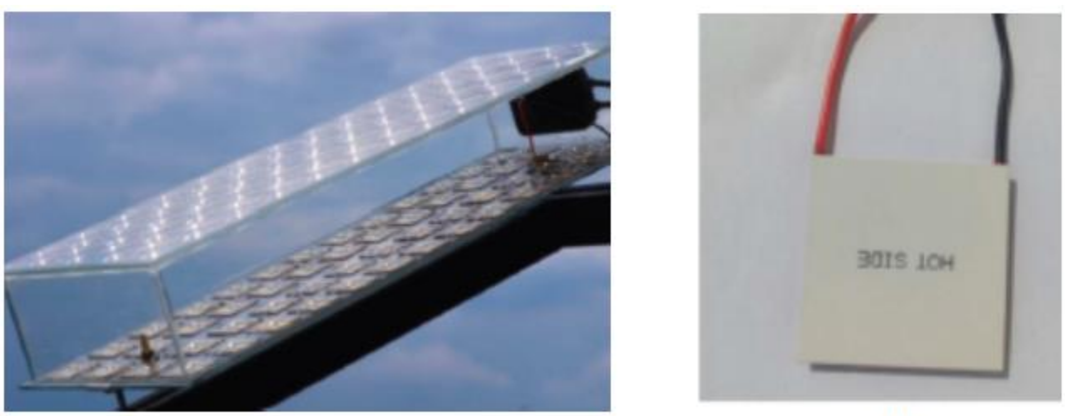

(a) (b)

Figure 1: (a) CPV cell with concentrator Fresnel lens and (b) commercial Bismuth telluride (Bi_2Te_3) TEG.

2. PHYSICAL MODEL

The current model consists of Fresnel lens used to concentrate incident solar spectrum on TJ photovoltaic solar which is composed of three cell layers stacked at the bottom of each other with GaInP followed by GaInAs and Germanium (Ge) layers the and connected to a circuit board of copper and ceramic layers, the cell layers are always substrated in the germanium layer which represent the active cell layer the cell dimensions and materials were referred to productive model of 10×10 mm^2 (type 3C44A) by AZURESPACE [6].

The cell bottom surface of solar cell was attached to the hot ceramic surface of thermoelectric generator with 98 thermoelectric legs of bismuth telluride varying between positive and negative connected by copper straps and covered from the top and bottom by ceramic layers which make a module of 49 thermoelectric couples thermally connected on parallel and electrically connected on series the whole hybrid system assembly is described in Figure 2 with the cell and thermoelectric generator dimensions described in Table 1 with TJ cell dimensions referred to [13] and TEG module to [14].

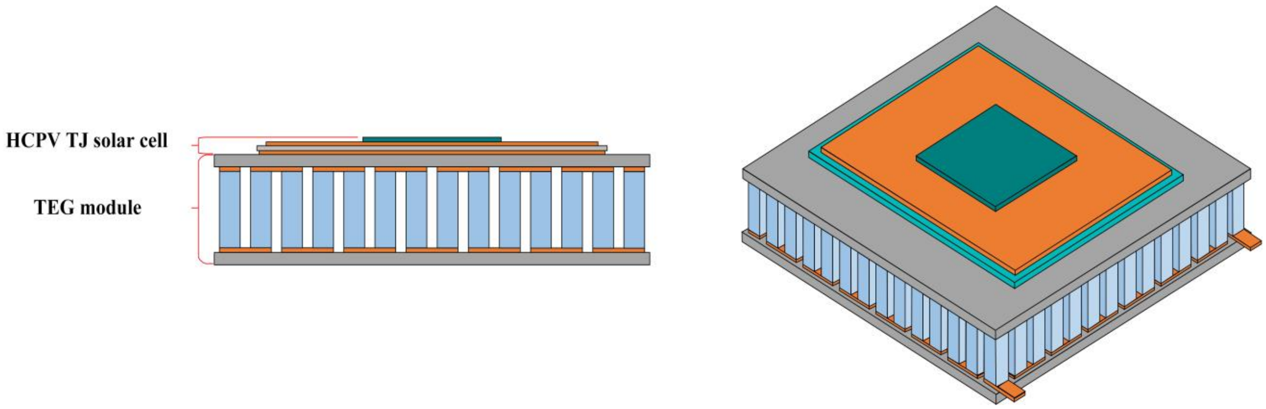

Figure 2: Hybrid TJ HCPV/TEG system assembly.

Table 1. Detailed dimensions of TJ cell and TEG parts.

Layer name		Length (L)	Width (W)	Thickness (t)
TJ cell	Germanium layer	10	10	0.19
	Upper copper	24	19.5	0.25
	Al_2O_3 ceramic	25.5	21	0.32
	Lower copper	25	20.5	0.25
TEG	Hot ceramic plate	31.5	31.5	0.8
	Copper strips	3.75	1.5	0.15
	P/N legs	1.5	1.5	5
	Cold ceramic plate	31.5	31. 5	0.8

*all dimensions on mm.

Table 2. The thermal and optical properties of both the TJ cell layers and heat sink materials.

	Material	k $\left(\frac{W}{m^2K}\right)$	c_p $\left(\frac{J}{kgK}\right)$	ρ $\left(\frac{kg}{m^3}\right)$	ε
TJ cell [13]	Germanium	60	320	5323	0.9
	Copper	400	385	8700	0.05
	Al_2O_3 ceramic	30	900	3900	0.75
TEG	Ceramic	35	837	3570	0.92
	Copper	385	400	8933	0.05
	Bismuth telluride (Bi_2Te_3)	[15]	544	7530	-

3. NUMERICAL SOLUTION

The solution undertook the following procedure, Firstly the material thermal and electrical properties are carefully defined; secondly, the model is created using Space claim software, thirdly mesh is created for each of model elements with an adequate number of elements, fourthly, the internal heat generation in the Germanium layer and the convection and radiation boundary conditions are defined to each surface of the module and finally the solution is applied using the predefined data.

The boundary conditions applied is mixed convection and radiation heat transfer for TJ cell germanium, copper and ceramic upper surfaces, and TEG ceramic upper surface. In contrast, the TEG cold ceramic bottom surface is exposed only to convection heat transfer, and an adiabatic boundary condition was applied on surfaces of TJ cell germanium, copper and ceramic layers and TEG ceramics, copper straps, and thermocouple legs side surfaces, the internal heat generation is only valid in the germanium cell layer and calculated by equation (1) [13].

$$\dot{q}'''_{Ge} = \frac{(1-\eta_{cell}) \cdot G \cdot \alpha_{Ge} \cdot A_{Ge}}{V_{Ge}} \tag{1}$$

Where η_{cell} is the cell electrical efficiency, G represents the incident concentrated solar radiation received by the Germanium cell in (W/m^2), the α_{Ge} gives the Germanium surface absorptivity, A_{Ge} is germanium surface area in (m^2) and V_{Ge} is the germanium layer volume in (m^3).

The TJ-Cell efficiency is calculated as a function of cell temperature due to its degradation with the increment in cell temperature and is given by equation (2) [16].

$$\eta_{cell} = \eta_{ref}\left(1-\beta_{ref}\left(T_{cell}-T_{ref}\right)\right) \tag{2}$$

with $\eta_{ref}$is the cell reference efficiency given by the cell producer [6] of 42.1 %, β_{ref} is temperature coefficient is cell temperature coefficient having the value of 0.047% [16] and T_{ref} is reference cell efficiency of 25 ℃, the convection heat transfer coefficient is given as a function of wind speed and is calculated using the following equation [17].

$$\mathrm{h_{conv}} = 5.82 + 4.07\ \mathrm{v_{wind}} \tag{3}$$

The overall hybrid system power output is calculated by

$$\mathrm{P_{sys.}} = \mathrm{P_{CPV}} + \mathrm{P_{TEG}} \tag{4}$$

Where P_{CPV} gives the TJ HCPV Cell power output given by equation (5) and P_{TEG} is the TEG power output given by equation (6)

$$P_{CPV} = \eta_{cell} \cdot G \cdot CR \cdot A_{Ge} \tag{5}$$

$$P_{TEG} = \left(\frac{n\ S\ (T_h - T_c)}{R_{in} + R_{load}}\right)^2 . R_{load} \tag{6}$$

Where n is the number of TEG thermocouples, S is the seebeck coefficient, $T_h$and T_c are the hot and cold ceramic temperatures, R_{in} is the TEG internal electrical resistance and R_{load} is connected load resistance [18], the maximum TEG power output is obtained when load resistance value is equal to TEG internal resistance $R_{in} = R_{load}$ [14].

1.1 MESH INDEPENDENCE TEST

To ensure that the simulation results are independent of the number of elements, a mesh independence test is applied to each configuration, and the number of elements is carefully chosen to preserve calculation time, mesh quality, and results from independence.

The test is applied on an uncooled MJ cell to test average cell temperature at the different number of elements, and as shown in Figure 3, the results showed no significant change in cell average temperature after number of an element of 6738 cells which is chosen as the applied element number for this model, and the same test was performed on a hybrid MJ/TEG system.

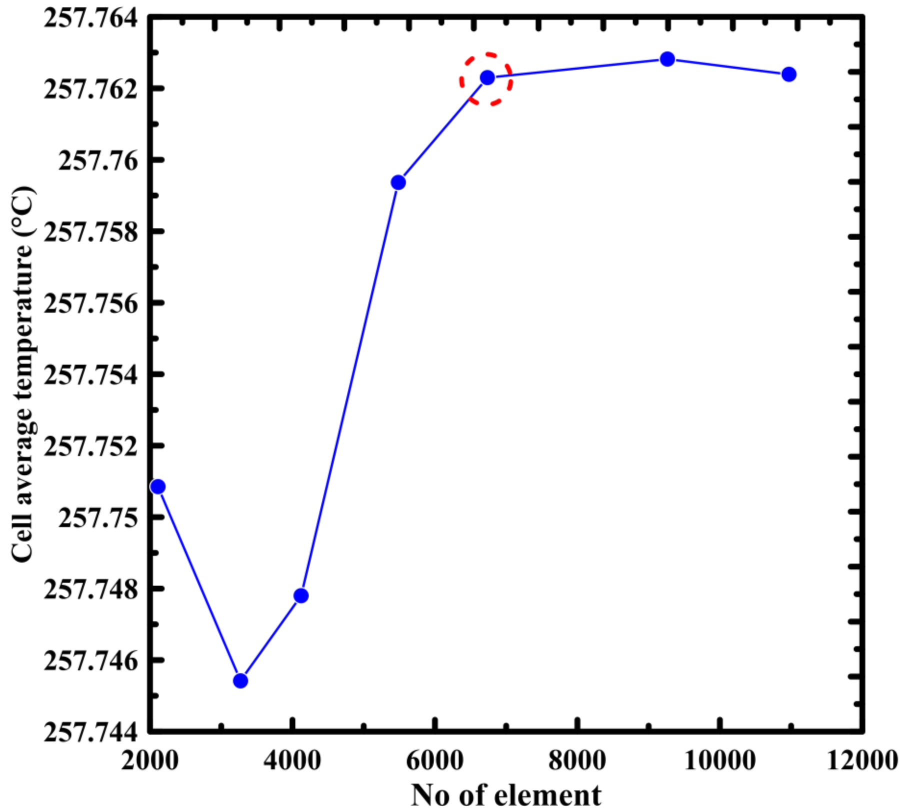

Figure 3: mesh independence test for MJ cell.

1.2 MODEL VALIDATION

The validation procedure determines whether or not the physical models used in CFD simulations are consistent with real-world conditions. The fundamental validation strategy identifies and quantifies the error by comparing simulation results to experimental or numerical solution data. As a result, the previously published triple-junction cell by Abo-Zahhad et al. [19] was simulated using the Ansys mechanical 3D thermoelectric model under the same conditions of the ambient temperature of 25 ℃ air velocity of 1 m/s, physical and thermal properties.

Figure 4 shows the resulting temperature at different solar concentration ratios for both Abo-Zahhad et al. [19] and the current simulation, highlighting the considerable convergence between results in both simulations with a maximum estimated error of 4.9% at a solar concentration ratio of 1000 suns.

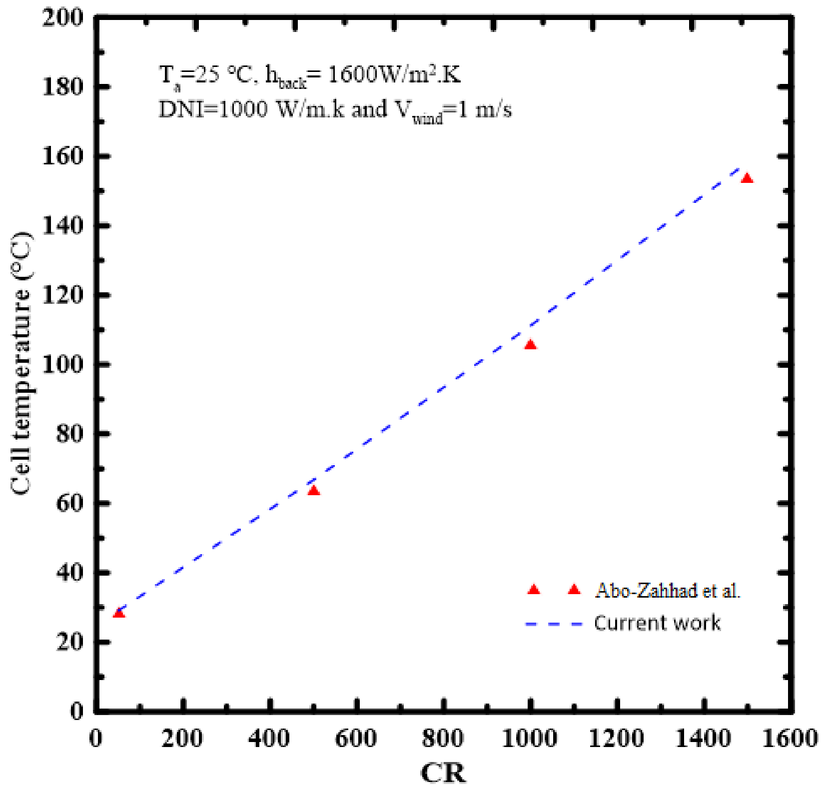

Figure 4: Comparison between solar cell temperature obtained by present CFD simulation and numerical results [17] versus solar radiation concentration ratios.

4. RESULTS AND DISCUSSION.

In this section, the effect of the combined cooling CPV / TEG system on the solar cell temperature, output power, and efficiency compared to the uncooled CPV, as shown in Figure 5, will be demonstrated. The simulation of the performance of the cooled CPV/TEG solar cell and uncooled solar cell under standard operating conditions of the ambient temperature of 25 °C, wind speed of 1 m/s, solar radiation of 1000 W/m^2, and with different concentrations of solar radiation, the following can be observed:

Figure 5 (a) depicts the variation in solar cell temperature for both uncooled TJ HCPV cells and hybrid TJ HCPV/TEG systems over a wide range of concentration ratios ranging from 5 to 50 suns. The maximum cell surface temperature for safe operation is 110 ℃ as recommended by the manufacturer [6] marked by the red line in the graph. It is noted that the uncooled cell can work under solar radiation up to 18.25 sun, after which the cell surface temperature increases higher than the permissible, and the cell is damaged. However, when the CPV is integrated with TEG, the solar cell temperature decreases at the same value of the solar concentration ratio compared to the uncooled CPV cell, allowing the hybrid CPV/TEG to operate at higher concentration ratios without exceeding the maximum permissible temperature limit. The maximum concentration ratios for the hybrid CPV/TEG reach 37.60 suns, representing a significant increase in the applied solar energy concentration.

The energy conversion efficiency in the cell is inversely proportional to the cell surface temperature, according to Equation (2). Figure 5 (b) depicts the efficiency variation for cooled and uncooled cells at different solar concentration ratios. The figure shows that the cell efficiency decreases gradually as the applicable solar concentration increases for both uncooled TJ HCPV and hybrid TJ/TEG systems.

By projecting the maximum limited concentration ratio of the uncooled TJ cell of 18.25 suns onto the efficiency curve, the maximum cell efficiency of 38.11% can be seen. At the exact value of solar concentration, the cooling cell system has an efficiency of about 40.16 %, and As the solar concentration ratios on the cell in hybrid system increase until they reach 37.60 suns, the efficiency drops to 38.12 %.

By applying equations from (4) to (6), it is possible to deduce the output electrical power obtained from both cooled and uncooled cells at different concentration ratios, as shown in Figure 5 (c).

Based on the previous figure, the maximum power output for uncooled cells is 0.695 W, as determined by projections of maximum operating concentration ratios for uncooled cells on the power curve. In comparison, the hybrid system achieves 0.733 W at the same solar concentration ratio of 18.25 suns but with a moderate operating temperature. By increasing the concentration ratio on the hybrid system to the maximum applicable value, the power output of the hybrid system reaches 1.433 W at a solar concentration ratio of 37.60 suns. On the other hand, the uncooled cell will not function under such conditions.

At the maximum performance conditions of the hybrid system, the TEG only contributed 0.03 % of the total system output, indicating that the TEG's role as a heat sink outperforms its effect as a power source. This diminished role of TEG as a power source is mainly due to low temperature gradient across the TEG hot and cold ceramics, As the TEG power output is directly proportional to the temperature gradient according to equation (6). As a result, it is advised that a cooling source be provided on the TEG cold ceramic in order to increase the system's power output.

Figure 6 depicts the temperature distribution across the TJ HCPV cell for both uncooled TJ HCPV and hybrid TJ HCPV/TEG systems at two solar concentrations of 15 and 35 suns. The temperature always has a peak value at the center of the germanium cell while decreasing gradually towards the terminals in both cases

the cooling effect of the hybrid, TJ HCPV/TEG is obvious at different solar concentration ratios, where at concentration ratios of 15 suns, the maximum surface temperatures of the MJ cell in hybrid system reaches 59.18 °C, compared to 94.58 °C as maximum cell temperature in uncooled TJ HCPV at the same conditions, as shown in Figure 6 (a) and (b).

While the cell surface temperatures rise when exposed to higher levels of solar radiation at 35 suns, as shown in Figure 6 (c) and (d), the hybrid system appears to be very close to the cell operation limits, with a maximum cell temperature of 104.21 suns, while the uncooled cell, when exposed to the same levels of solar radiation, would not operate cause the cell temperature would rise to 189.39 °C, which is higher than the factory limit, and thus the cell may be damaged.

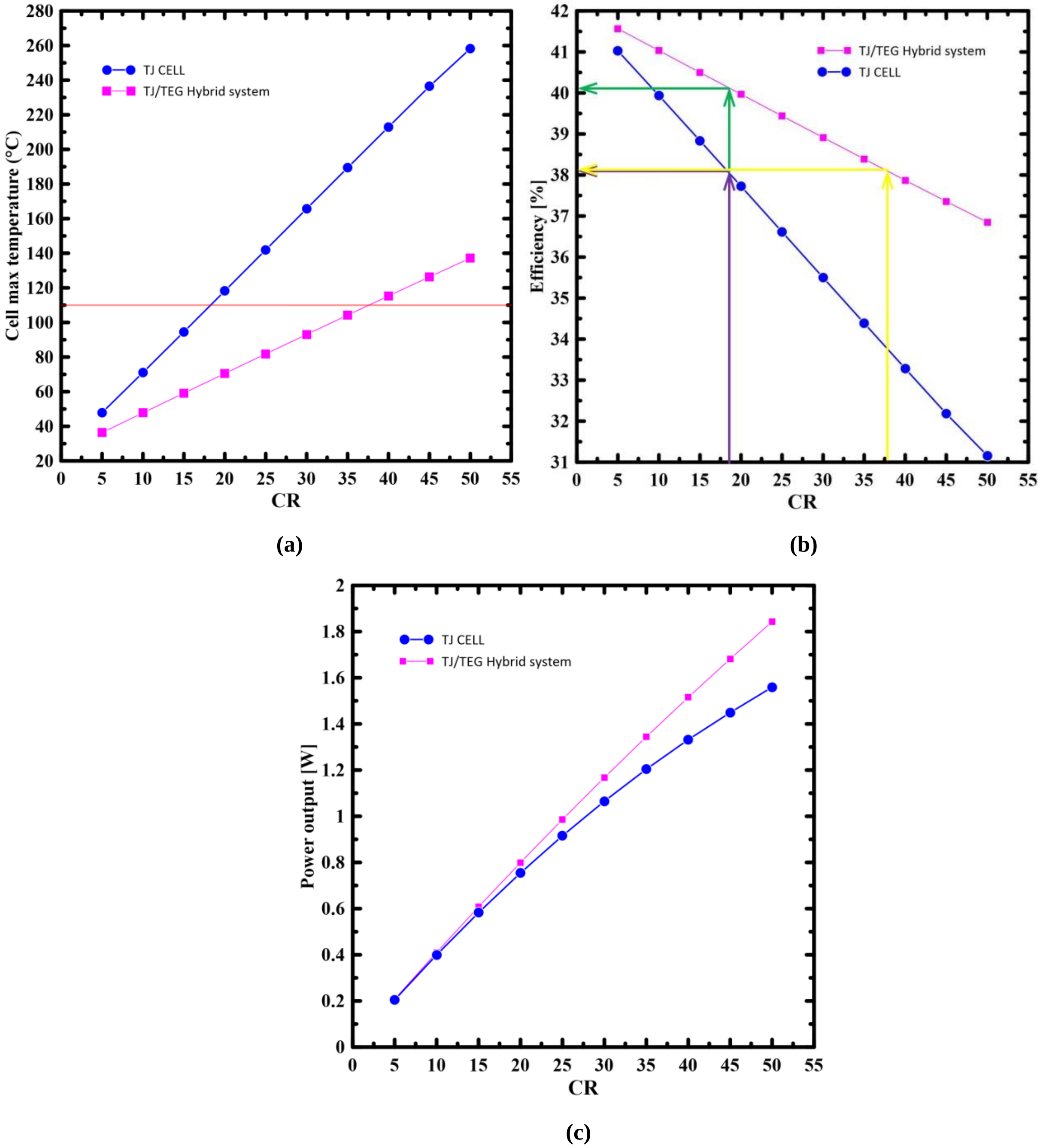

Figure 5: The performance of the TJ/TEG hybrid system versus uncooled cells at different radiation concentrations is represented in (a) solar cell temperature, (b) electrical efficiency, and (c) output power.

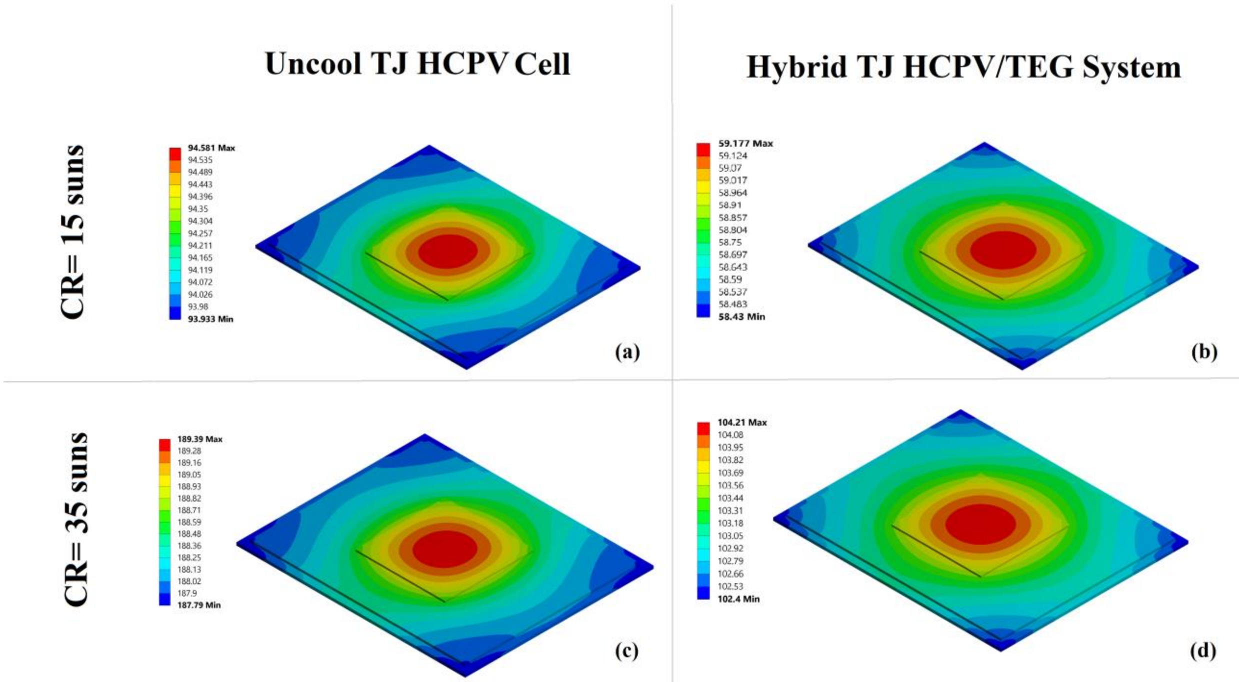

Figure 6: Temperature distribution on the cooled and uncooled cell surfaces at two different radiation concentrations (a) CR=15 suns and (b) CR=35 suns.

5. CONCLUSIONS

This study compared the performance of passive cooling of TJ HCPV cells employing TEG to create a hybrid system, and the hybrid system was tested under different solar concentration ratios at the same ambient temperature and wind speed against the uncooled TJ cell, At the maximum operating concentration for the uncooled cell of 18.25 suns, the cell temperature was decreased in the hybrid system to reach 66.58 °C under the same solar concentration, with an increase in power output of 5.47 % and an improvement in the system overall electrical efficiency of 10.45 %., In addition, the hybrid boosted the highest applicable concentration ratio to 37.60 suns, with an overall system power output of 1.433 W/cm^2. Thus, the TEG presence in the bottom of the CPV cell created a passively cooled hybrid power generation system, however its role in cooling the cell outperforms that of power generation.

Nomenclature

Symbol	Description	Symbols	Description
Roman			
A	Area (m^2)	Ceramic	ceramic layer
c_p	specific heat capacity at constant pressure (J/kg · K)	cu-lower	lower copper layer
		cu-upper	upper copper layer
G	solar irradiance (W/m^2)	Ge	Germanium cell
g	gravitational acceleration (m/s^2)	Max	Maximum
$\dot{q}'''$	heat generation per unit volume (W/m^3)	Ref	reference
$\dot{q}$	heat transfer rate (W)	Sc	solar cell
$\dot{q}''$	heat flux (W/m^2)	Bi_2Te_3	Bismuth telluride
T	Temperature (°C)	**Abbreviations**	
T_{amb}	Ambient air temperature (°C)	CPV	concentrator photovoltaic
V	volume (m^3)	CR	concentration ratio (suns)
v_{wind}	wind speed (m/s)	Ge	germanium
h_{conv}	Convection heat transfer coefficient (W/m^2.°C)	HCPV	High concentrator photovoltaic
S	seebeck coefficient (V/K)	MJ	multijunction
Greek		Mm	millimeter
A	Absorptivity	PV	photovoltaic
β_{rel}	relative cell efficiency temperature coefficient (K^{-1})	SJ	single junction
E	Emissivity	TJ	triple junction
Subscripts		TEG	Thermoelectric generator
Amb	ambient air		
Al	Aluminum		

6. REFERENCES

[1] Ju X, Xu C, Hu Y, Han X, Wei G, Du X. A review on the development of photovoltaic/concentrated solar power (PV-CSP) hybrid systems. Sol Energy Mater Sol Cells 2017;161:305–27. https://doi.org/10.1016/j.solmat.2016.12.004.

[2] Sripadmanabhan S, Aravind C, Chong K, Saidur R, Faizal M, Abubakar S, et al. A review on various configurations of hybrid concentrator photovoltaic and thermoelectric generator system. Sol Energy 2020;201:122–48. https://doi.org/10.1016/j.solener.2020.02.090.

[3] Philipps SP, Dimroth F, Bett AW. High-efficiency III-V multijunction solar cells. McEvoy's Handb. Photovoltaics Fundam. Appl., Academic Press; 2018, p. 439–72. https://doi.org/10.1016/B978-0-12-809921-6.00012-4.

[4] Sathe TM, Dhoble AS. A review on recent advancements in photovoltaic thermal techniques. Renew Sustain Energy Rev 2017;76:645–72. https://doi.org/10.1016/j.rser.2017.03.075.

[5] LightandLife-IYL_Proceedings2016.pdf n.d.

[6] Azure Space Solar Power GMBH. Enhanced Fresnel Assembly - EFA Type: 3C42A – with 10x10mm^2 CPV TJ Solar Cell Application: Concentrating Photovoltaic (CPV) Modules 2014:0–4.

[7] N.M. Ravindra, Bhakti Jariwala, Asahel Bañobre AM. Thermoelectrics Fundamentals , Materials Selection , Properties , and Performance. n.d.

[8] Liao M, He Z, Jiang C, Fan X, Li Y, Qi F. A three-dimensional model for thermoelectric generator

and the influence of Peltier effect on the performance and heat transfer. Appl Therm Eng 2018;133:493–500. https://doi.org/10.1016/j.applthermaleng.2018.01.080.

[9] Liao T, Lin B, Yang Z. International Journal of Thermal Sciences Performance characteristics of a low concentrated photovoltaic e thermoelectric hybrid power generation device. Int J Therm Sci 2014;77:158–64. https://doi.org/10.1016/j.ijthermalsci.2013.10.013.

[10] Sabry M, Lashin A, Al M. Journal of King Saud University – Science Experimental and simulation investigations of CPV / TEG hybrid system. J King Saud Univ - Sci 2021;33:101321. https://doi.org/10.1016/j.jksus.2020.101321.

[11] Deng Y, Zhu W, Wang Y, Shi Y. Enhanced performance of solar-driven photovoltaic – thermoelectric hybrid system in an integrated design. Sol Energy 2013;88:182–91. https://doi.org/10.1016/j.solener.2012.12.002.

[12] Beeri O, Rotem O, Hazan E, Katz EA, Braun A, Gelbstein Y. Hybrid photovoltaic-thermoelectric system for concentrated solar energy conversion: Experimental realization and modeling. J Appl Phys 2015;118. https://doi.org/10.1063/1.4931428.

[13] Zaghloul H, Emam M, Abdelrahman MA, Abd Rabbo MF. Optimization and parametric analysis of a multi-junction high-concentrator PV cell combined with a straight fins heat sink. Energy Convers Manag 2021;243:114382. https://doi.org/10.1016/j.enconman.2021.114382.

[14] Abdo A, Ookawara S, Ahmed M. Performance evaluation of a new design of concentrator photovoltaic and solar thermoelectric generator hybrid system. Energy Convers Manag 2019;195:1382–401. https://doi.org/10.1016/j.enconman.2019.04.093.

[15] Shen ZG, Wu SY, Xiao L, Yin G. Theoretical modeling of thermoelectric generator with particular emphasis on the effect of side surface heat transfer. Energy 2016;95:367–79. https://doi.org/10.1016/j.energy.2015.12.005.

[16] Abo-Zahhad EM, Ookawara S, Radwan A, El-Shazly AH, Elkady MF. Numerical analyses of hybrid jet impingement/microchannel cooling device for thermal management of high concentrator triple-junction solar cell. Appl Energy 2019;253:113538. https://doi.org/10.1016/j.apenergy.2019.113538.

[17] Rabie R, Emam M, Ookawara S, Ahmed M. Thermal management of concentrator photovoltaic systems using new configurations of phase change material heat sinks 2019;183:632–52.

[18] Lee H, editor. Thermoelectrics: Design and Materials. Chichester, UK: John Wiley & Sons, Ltd; 2016. https://doi.org/10.1002/9781118848944.

[19] Abo-Zahhad EM, Ookawara S, Radwan A, El-Shazly AH, El-Kady MF, Esmail MFC. Performance, limits, and thermal stress analysis of high concentrator multijunction solar cell under passive cooling conditions. Appl Therm Eng 2020;164:114497. https://doi.org/10.1016/j.applthermaleng.2019.114497.